PHYSICAL REVIEW B **82**, 054433 (2010)

Resonant magnetic reflectivity in the extreme ultraviolet spectral range: Interlayer-coupled Co/Si/Ni/Fe multilayer system

P. Grychtol,[1] R. Adam,[1] S. Valencia,[2] S. Cramm,[1] D. E. Bürgler,[1] and C. M. Schneider[1]
[1]*Institute of Solid State Research, IFF-9, Forschungszentrum Jülich, D-52425 Jülich, Germany*
[2]*Helmholtz-Zentrum-Berlin, BESSY, Albert-Einstein-Strasse 15, D-12489 Berlin, Germany*
(Received 18 May 2010; published 30 August 2010)

A polycrystalline test structure comprising a 5 nm cobalt and a 10 nm nickel/iron layer separated by a silicon layer ranging from 1.5 to 4 nm prepared by thermal evaporation has been investigated by resonant magnetic reflectivity measurements of horizontally polarized light in the extreme ultraviolet spectral range. By exploiting the transversal magneto-optical Kerr effect at the *M* absorption edges of cobalt and nickel (59.5 eV and 66.5 eV) a magnetic contrast as large as 80% for cobalt and 25% for nickel can be obtained near a Brewster angle of about 45°. Angle- and energy-dependent scans of the magnetic asymmetry as well as element-selective, magneto-optical loops of the hysteresis were recorded against the thickness of the interlayer, reflecting the switching behavior of the individual ferromagnetic layers as a function of the interlayer coupling.

DOI: 10.1103/PhysRevB.82.054433 PACS number(s): 75.25.−j

I. INTRODUCTION

The interaction of light with a magnetic system provides a wealth of experimental information to study various aspects of magnetism. An example is the magneto-optical Kerr effect (MOKE), which denotes the elastic scattering of polarized light at a magnetic surface within the visible range. Here, a change in the magnetization state in the material usually induces a change in the polarization state of the scattered light, except for a transversal Kerr (T-MOKE) geometry, in which the magneto-optical response directly translates into an intensity modulation. Exploiting MOKE in a reflectivity experiment is a well-established technique for investigations of static and dynamic processes in magnetism.[1–3] At wavelengths above 250 nm, however, the effect is weak in most materials—less than a millirad of Kerr rotation and far below a percent change in intensity upon a full magnetization reversal. Furthermore, wavelengths employed in conventional MOKE experiments are large as compared to cutting-edge magnetic structures on the nanometer scale, thus precluding their imaging with an appropriate lateral resolution.[4]

In the last decades, these shortcomings have been largely overcome by exploiting much stronger magneto-optical effects in the soft x-ray regime. Although these effects can be treated in a common theoretical framework, it is convenient to distinguish between magnetodichroic phenomena in absorption and transmission, i.e., x-ray magnetic circular dichroism (XMCD) and linear dichroism, and magnetodichroic effects in reflection, which are often grouped under the term x-ray resonant magnetic scattering (XRMS). All of these phenomena require a resonant excitation by means of linearly or circularly polarized tunable soft x rays. Access to this radiation is provided by large synchrotron radiation facilities, which significantly increases the experimental complexity as compared to a laboratory approach. By exploiting XRMS and XMCD effects at the *L* edges of transition metals at photon energies above 500 eV, not only a superior magnetodichroic contrast of up to several tens of percent and a lateral resolution down to a few nanometers can be attained, but also element and chemical selectivity can be gained in a resonant excitation.[5–7] These x-ray magneto-optical phenomena allow for magnetic investigations of individual constituents of heterogeneous ferromagnetic systems on a nanometer and on a femtosecond scale, if suitable light sources such as free-electron lasers[8] or appropriate techniques such as femtoslicing[9] are employed.

So far, only few experiments have addressed resonant magnetic reflectivity and magnetic dichroism at the *M* edges of transition metals at photon energies around 50 eV—in the extreme ultraviolet (XUV) regime. In terms of the magneto-optical response, these XUV phenomena have been found equally useful, with changes in the dichroic contrast ranging up to almost 100%.[10–14] Because the majority of beamlines at third-generation synchrotron facilities are dedicated to photon energies in the soft x-ray region, the opportunity of XUV magneto-optical studies has mostly escaped the attention of the magnetic community. However, recently substantial progress has been made in laser-based light sources reaching photon energies of up to 100 eV with moderate effort justifying a closer look into XUV magneto-optics. Advancements in laser amplifier technology have brought about reliable table-top light sources, which are able to produce coherent and ultrashort XUV light pulses exploiting a highly nonlinear conversion process (higher harmonic generation—HHG).[15–17] Due to the pulsed and coherent nature of the emitted radiation, HHG-based light sources may serve as compact tools for element-selective investigations of magnetic properties on the femtosecond and nanometer scale in a laboratory environment.[18,19]

For this reason, we present in this contribution magneto-optical studies in the XUV performed with synchrotron radiation at the *M* edges of ferromagnets, which are based on transition metals in a spin-valve-type layered system. We explore advantages and disadvantages of experiments in this spectral range and discuss the data as a basis for future studies employing HHG-based table-top systems.

II. XUV VS SOFT X-RAY REGIME

The XUV spectral range offers certain advantages over the soft x-ray regime with respect to magneto-optical studies.

Several experiments have already shown that magnetic investigations of single films by resonantly scattered XUV light at the *M* absorption edges of transition metals[10–14] and the *N* absorption edges of the lanthanide series[20,21] yield very strong magnetodichroic signals. Moreover, studies of the Faraday rotation and the Voigt effect at the *M* and *L* absorption edges of Fe, Co, and Ni reveal that magneto-optical constants and thus responses at the *M* edges are as large as those at the *L* edges. This fact emphasizes the dominant role of the exchange interaction in comparison to the spin-orbit coupling in the generation of magnetic contrast at the *M* edges.[14,22,23] It is the high absorbance of most materials, at angles where the magnetodichroic signal in the XUV maximizes, which gives no rise to a magnetic contrast in comparable soft x-ray experiments. In a T-MOKE geometry, the maximum of the magnetodichroic response is located around the Brewster angle, i.e., incoming and outgoing light beam enclose an angle of $\sim 90°$. Under these conditions, there is still a sizable reflectance on the order of $R \sim 10^{-4}$, which ensures a reasonable signal-to-noise ratio in the XUV. In the soft x-ray regime, on the other hand, the light penetrates deeper into the sample and the reflectivity drops off much faster with increasing incidence angle θ, reaching values of $R \sim 10^{-10}-10^{-11}$ at $\theta=45°$.[24] Therefore, in the soft x-ray regime grazing incidence optics are required adding to the complexity of the experimental setup. This also generates a considerable problem for imaging experiments in a reflection geometry, as the focusing of the photon beam becomes very difficult and the imaged plane is not well defined. That is why a right-angle geometry, generally favored in the XUV, is much more suitable for imaging experiments. This approach is sensitive to the in-plane magnetization in contrast to transmission techniques in the soft x-ray regime, which are only sensitive to the magnetic out-of-plane component, thus imposing certain restrictions on the sample thickness and the geometry with respect to the probe beam.

Another aspect concerns optical interference effects arising in the sample. Typical structural dimensions of a sample system, such as the individual layer thickness in a multilayer stack, and the wavelength corresponding to a transition-metal *L* edge are of a similar magnitude, i.e., on the order of a few nanometer (1.59 nm for Co L_3 absorption edge at 778.1 eV). In a reflectivity experiment at these photon energies, the multilayer acts as a superlattice, resulting in a relatively complex interference pattern mixing structural and magnetic periodicities. As a consequence, the reflected intensity exhibits a strong angular modulation of the magnetodichroic signal and structural and magnetic properties cannot be separated easily.[25] In the case of *M* edges, where the wavelength is one order of magnitude larger (20.6 nm for Co *M* absorption edge at 60.2 eV), structurally induced interferences in the magnetic signal are less pronounced, simplifying the interpretation in this respect. For the same reason, surface and interface roughness influence the magnetic signal to a much smaller extent. Moreover, due to a smaller penetration depth of the XUV radiation, Kiessig fringes—resonances between surface and substrate—do not occur, further facilitating the interpretation.

Just as the XUV region of the electromagnetic spectrum is located in between the visible and soft x-ray range, its interaction with matter combines the characteristics of both spectral regions. This makes XUV light a unique element-selective, ultrafast probe of magnetism on the nanometer scale, which is going to be available in any optical laboratory in the near future. Since only little attention has been paid to the XUV region, it is the purpose of this work to explore its potential as a magnetic contrast mechanism by tuning the photon energy to the *M* absorption edges of Co and Ni in a T-MOKE reflectivity experiment and focusing on layer-selective investigations of magnetically coupled multilayer systems.

III. SAMPLE

The sample consisted of a magnetic trilayer structure and was prepared by thermal evaporation at a base pressure of 5×10^{-11} mbar.[26] In a first step, a substrate system for the magnetic multilayer was manufactured comprising a 150-nm-thick Ag(001) buffer layer,[27] which was grown on an iron precovered GaAs(001) wafer at a temperature of 380 K. After postannealing at a temperature of 570 K, a 2 nm Fe followed by a 8 nm Ni layer were deposited onto the buffer at room temperature. A stepped Si layer with a step height of 1.5, 2.5, and 4 nm, each 1 mm wide, followed. Finally, a 5-nm-thick Co layer was deposited on top.

The magnetic switching behavior in the plane of the multilayer system was first characterized by MOKE measurements in the visible range.[28] Recording hysteresis loops in a longitudinal MOKE (L-MOKE) setup for various angles of the sample with respect to the external magnetic field revealed a negligible magnetocrystalline anisotropy. Three regions of different interlayer coupling between the ferromagnetic Co and Ni/Fe layers were identified and associated with regions of different Si spacer thicknesses, as deduced from distinct coercivities of the hysteresis loops, which are displayed in Fig. 1.

As can be seen from this figure, at a spacer thickness of 1.5 nm the multilayer is ferromagnetically coupled forcing all layers to switch simultaneously. At a spacer thickness of 4 nm, the multilayer is entirely decoupled allowing for an independent switching of the top Co and bottom Ni/Fe layers. Independent experiments prove that the Ni/Fe bilayer indeed behaves like a single magnetic unit. At a spacer thickness of 2.5 nm, an intermediate behavior can be observed, in which the reversal of one layer is hindered by a weak ferromagnetic interlayer coupling. The hysteresis loops taken in the visible range do not reveal directly, which layer switches first, thereby necessitating a layer- and element-selective approach.

IV. EXPERIMENTAL SETUP

In order to further characterize the magnetic multilayer, we performed resonant magnetic reflectivity measurements in a T-MOKE geometry at the undulator beamline UE56/1-SGM of the synchrotron radiation facility BESSY II. The reflectivity of linearly *p*-polarized XUV light was measured across the *M* absorption edges of Co and Ni from 57 to 72 eV with an energy resolution of 0.1 eV and a degree of linear

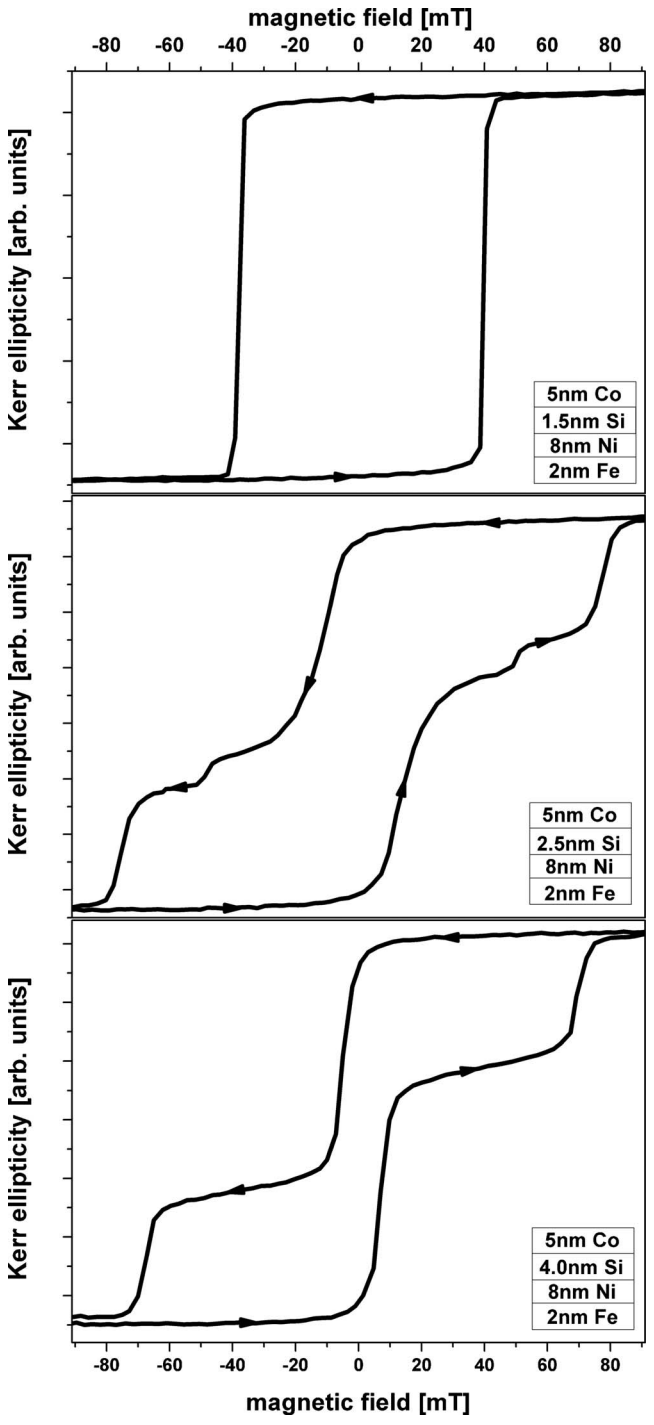

FIG. 1. Magneto-optical loops of the multilayer wedge system taken at a Si spacer thickness of 1.5 nm (top), 2.5 nm (middle), and 4 nm (bottom) by means of a longitudinal MOKE setup.

polarization exceeding 99%. The lower photon energy limit of 57 eV was determined by the smallest possible gap of the undulator forcing us to omit the Fe M absorption edge located around 54 eV in our studies. Horizontal and vertical focusing mirrors enabled the synchrotron beam to be focused down to a spot size of approximately 100×100 μm^2 at the sample surface.

The multilayer stack was placed into a dedicated ultrahigh vacuum reflectometer allowing for θ-2θ scans in a horizontal plane with the angle of incidence θ ranging from 0° to 90°. The intensity of the XUV light reflected off the sample was detected by a Schottky-type GaAsP photodiode (Hamamatsu—G1127) directly connected to a sensitive amperemeter (Keithley–6517A). The photodiode was covered by a 200-nm-thick Al filter blocking out laser light emitted from a pulsed Ti:Sapphire laser (Femto Lasers—Synergy), which was introduced to excite the sample for element-selective studies of precessional magnetization dynamics.[29] The absorption edge of the Al filter located at 72 eV determined the higher photon energy limit of our study. A set of vertically mounted coils was capable to generate a static magnetic field of up to ± 140 mT.

V. THEORETICAL CONSIDERATIONS

In order to extract information about the sample magnetization in MOKE experiments in the visible range, changes in the polarization state of the reflected light are usually analyzed in a polar or longitudinal geometry. In contrast to this, most resonant magnetic reflectivity experiments in the XUV and soft x-ray region already provide information about the magnetic state of the sample via a magnetically induced change in the reflected intensity, i.e., a magnetodichroic signal. Its strength originates from a large resonant enhancement of the reflected light if the energy of the incident beam is tuned to the absorption edges of the material under investigation.[30] This strongly resonant behavior involves low-order electric multipole transitions between core levels and unoccupied states of the valence band which results in both element selectivity and magnetic sensitivity in the presence of spin-orbit coupling and exchange interaction. In a simple picture, the magnetic sensitivity originates from the interplay of two mechanisms. First, the exchange interaction energetically splits the magnetic sublevels m_J of both the upper and lower state which are involved in the photoexcitation process.[31] This results in spin-split core states and a spin-split density of the valence states. Second, the spin-orbit coupling in either the lower or the upper state (or in both) causes the optical interband transitions to become spin dependent, which is also known as optical spin orientation.[32] As these spin-dependent interband transitions excite the electron into an already spin-polarized empty state, the strength of the transition matrix element for transitions from each sublevel m_J is now determined by both the magnetization direction and the light polarization, resulting in a magneto-optical response. For $3d$ transition metals, enhanced magnetic resonances occur at $L_{2,3}$ absorption edges in the range of 650–950 eV and at the $M_{2,3}$ absorption edges in the range of 50–75 eV by involving mainly $2p \rightarrow 3d$ and $3p \rightarrow 3d$ transitions, respectively. For $4f$ systems, strong resonant magnetic scattering occurs at the $N_{4,5}$ absorption edges in a range of 100–190 eV related to predominantly $4d \rightarrow 4f$ transitions.

As the reflected signal comprises the response of the charge system mainly involving dipole transitions as well as the response of the magnetic system mainly involving quadrupole transitions, the magnetic state of the sample has to be derived from the change in the reflectivity as a function of an applied magnetic field. In the following, we will focus our

attention to a T-MOKE geometry, which has been adopted in our resonant scattering experiments described below. The strength of the T-MOKE signal, being odd in magnetization **M**, is commonly denoted as the normalized difference of the reflected intensity I for two inverted directions of the sample magnetization, here referred to as $\uparrow$ and $\downarrow$. The latter can be achieved by an external magnetic field applied transversely to the scattering plane. This so-called magnetic asymmetry A is related to the Fresnel reflection coefficients within the classical magneto-optical formalism,[33]

$$A = \frac{I_\uparrow - I_\downarrow}{I_\uparrow + I_\downarrow} = \frac{|r_{pp}^\uparrow|^2 - |r_{pp}^\downarrow|^2}{|r_{pp}^\uparrow|^2 + |r_{pp}^\downarrow|^2}.$$

Its maximum is close to the Brewster angle, where in a simplified picture for p-polarized light the oscillation axis of the electric dipole coincides with the axis of specular reflection along which no dipole radiation is emitted. Due to the distinct emission characteristic of the multipole radiation, for this angle the response of the charge system is suppressed, whereas the magnetic contribution resulting from the quadrupol transitions prevails. Thus, the magnetic contribution dominates the total signal.

The reflection coefficient r_{pp}, consisting of a nonmagnetic r_{pp}^0 and a magnetic Δ_{pp} response, describes the influence of materials on p-polarized light which is incident at an angle of θ_i and reflected at an angle of θ_r, with n_0 being the refractive index of the nonmagnetic transmitted medium and $\bar{n}$ being the average refractive index of the magnetic reflective medium,[34]

$$r_{pp}^{\uparrow\downarrow} = r_{pp}^0 \pm \Delta_{pp} = \frac{\bar{n}\cos\theta_i - n_0\cos\theta_r}{\bar{n}\cos\theta_i + n_0\cos\theta_r} \pm \frac{2in_0\bar{n}\cos\theta_i\sin\theta_r}{(\bar{n}\cos\theta_i + n_0\cos\theta_r)^2} Q_x.$$

In isotropic media, the Voigt vector **Q**, being directly related to the dielectric tensor and commonly introduced to account for magnetic interactions, is linearly proportional to the magnetization **M** and points in its direction, here along the x axis, which is perpendicular to the plane of incidence. As the formulation above is directly deduced from Maxwell's equations utilizing boundary conditions for dielectric media within a magneto-optical framework, it can be readily applied to resonant reflectivity from multilayer structures in the XUV and soft x-ray region. In order to interpret the experimental data, the magneto-optical response of the multilayer under investigation has also been simulated by a computer code based on a 4×4 matrix formalism, which also takes into account interference effects as well as surface and interface roughness.[25]

VI. RESULTS AND DISCUSSION

A. XUV magneto-optical response

As a first step in the experiment, we determined the conditions for a maximum of the magneto-optical signal. For this purpose we mapped the magnitude of the dichroism by taking angular and photon energy scans of the magnetic asymmetry. These measurements were performed for regions

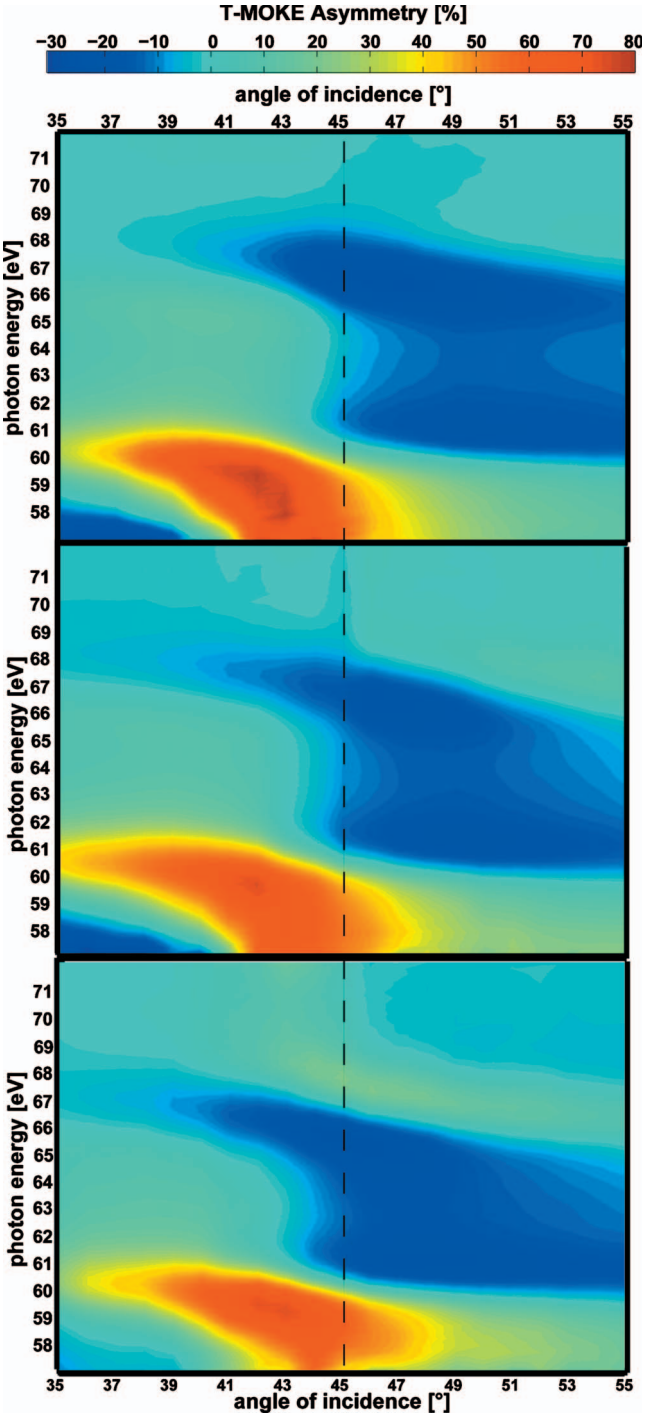

FIG. 2. (Color) Angular- and energy-dependent magnetic asymmetry of the multilayer wedge system taken at a Si spacer thickness of 1.5 nm (top), 2.5 nm (middle), and 4 nm (bottom).

of different interlayer coupling clearly identified previously in the visible range. For each of these three regions, Fig. 2 depicts the measured asymmetry across the Co and Ni edge in an energy range of 57–72 eV with the angle of incidence θ varying from 35° to 55° and a magnetic field reversing between ±100 mT, thereby magnetically saturating the sample in opposite directions.

At a first glance, the overall appearance of the asymmetry distributions $A(\theta, h\nu)$ for different Si interlayer thicknesses is

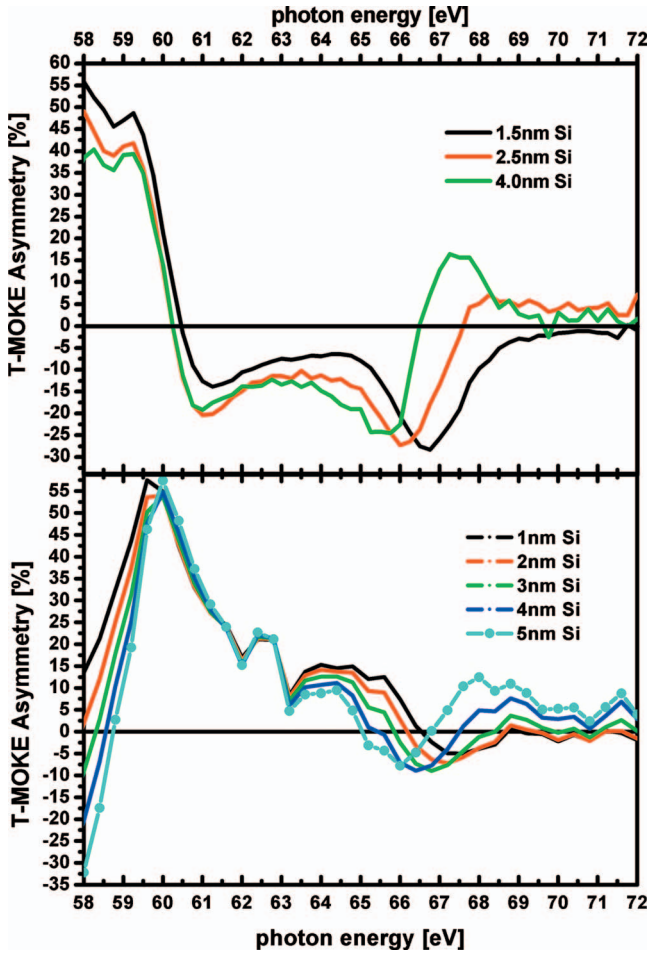

FIG. 3. (Color) Measured (top) and calculated (bottom) T-MOKE asymmetry spectra of the multilayer wedge system for a fixed incidence angle of 45° and various Si spacer thicknesses.

quite similar. A closer inspection, however, reveals distinct differences between the magneto-optical signal associated with the absorption edges of Co and Ni. As the main spectral feature, a pronounced bipolar peak structure can be identified in the asymmetry distribution at an energy of 59.5 eV (61 eV) and an angle of 42° (50°) with an amplitude of about 80% (−25%) in all three regions of the stepped wedge system. This feature can be clearly attributed to the resonant excitation of the Co at the M absorption edge and it is consistent with earlier findings.[10] A totally different behavior of the asymmetry $A(\theta, h\nu)$ can be observed at the M absorption edge of Ni. At the lowest Si interlayer thickness (top graph), the magnetic asymmetry has only a dip shape with a negative extremum of about −25% at an energy of 66.75 eV and an angle of 47°. With increasing spacer thickness, the resonance moves toward an energy of 65.5 eV (67.5 eV) and an angle of 45° (46°). At the same time, it also changes its shape to a bipolar resonance with an overall amplitude of about ±20%.

In an effort to further exemplify and elaborate on this behavior, we have calculated magnetic asymmetry spectra $A(h\nu)$ for all three sample configurations using the formalism mentioned above.[25] The calculation has been carried out for a fixed angle θ of 45°. This position is marked by a dashed line in Fig. 2, along which corresponding experimental spectra have been extracted. The calculated spectra are compared to the experimental data in Fig. 3.

The experimental data for various Si interlayer thicknesses (black, red, and green curve) are compiled in the top graph of Fig. 3. From these curves we again discern clear differences for the spectral ranges related to Co and Ni. We find that the measured asymmetry below 59.5 eV remains at around 45% for all three regions with a tendency to decrease for increasing Si spacer thicknesses. The curves drop sharply and simultaneously to about −20% at 61 eV, leveling off with increasing photon energy at approximately −10%. This magneto-optical response indicates that the Co top layer behaves magnetically and optically similar in all three samples. Clearly, changes in the asymmetry induced by the spacer thickness happen to occur in the vicinity of 67 eV, where we observe strong variations in the shape and energy position of the spectral features. No magnetic signal can be found above 70 eV.

The colored curves in the bottom graph of the same figure represent the calculated asymmetry spectra for this multilayer system based on optical constants taken from Henke[24] and magneto-optical constants extracted from previously measured rotation spectra.[14] Furthermore, we have neglected surface and interfacial roughness in this calculation, since previous simulations have proven them to play a minor role in the response of the multilayer. As the Si interlayer thickness may have deviations from the nominal value, we have calculated the magneto-optical response for several interlayer thicknesses ranging from 1 to 5 nm. The simulation results indicate a clear trend with respect to the spectral behavior. The Co-related signal is almost independent of the interlayer thickness, whereas the Ni-related features exhibit a clear modulation. With increasing Si interlayer thickness, the Ni signal becomes more pronounced and its features shift toward lower photon energies. In particular, the transition from an unipolar to a bipolar resonance is clearly visible. Most of these trends are qualitatively reproduced by the experimental data in a very reasonable manner. The strong deviation in the energy range of 61–65 eV can be explained by relatively noisy data of the before-mentioned rotation spectra taken to extract the magneto-optical constants, which are the basis of our simulations—see Fig. 5 in Ref. 14. Nonetheless, the qualitative good agreement between the calculated and the measured magneto-optical response of the multilayer at the Ni edge suggests that the observed shift can be related to interferences of the reflected XUV light at the interfaces of the multilayer stack. We also note a characteristic trend at photon energies below 60 eV. With increasing Si thickness the signal drops and even changes sign. This is related to the response of the buried Fe layer, whose response we were not able to access entirely in our study because of the limited spectral range. However, the trend is somewhat visible in the experimental curves, although the effect is much smaller. This deviation is most likely related to the low photon flux and thus bad signal-to-noise ratio introducing a relatively high uncertainty in the absolute value of the asymmetry below 58 eV. At these photon energies, the undulator gap reaches its minimum and it cannot be reliably synchronized with the monochromator any further.

B. Magnetic switching behavior

Having identified maxima of the magnetic contrast at the *M* absorption edges of Ni and Co, the incidence angle and photon energy can be tuned to probe the magnetic switching behavior element selectively, which in the case of a multilayer system translates into a layer-specific response. For this purpose, we have recorded the magnetic field dependence of the magneto-optical signal $A(\mu_0 H)$. This measurement results in hysteresislike loops which do not, however, directly reflect the behavior of the magnetization, as the signal comprises a convolution of magnetic and optical contributions. We will therefore call them *magneto-optical loops*. The loops, which are displayed in red and green in Fig. 4, have been recorded at a fixed angle of 41°, where local, element-specific maxima of the magnetic contrast are clearly separated, for reasons that are explained further below. The response at the Co edge was taken at a photon energy of 59.5 eV for all three regions (red curves), whereas the response at the Ni edge was recorded at a photon energy of 67.5 eV for a 1.5 nm Si spacer, at a photon energy of 67 eV for a 2.5 nm Si spacer, and at a photon energy of 66.5 eV for a 4 nm Si spacer (green curves). These data are compared to the conventional Kerr loops in Fig. 1.

The top graph in Fig. 4 shows magneto-optical loops associated with a sample region having a Si spacer thickness of 1.5 nm. All three loops exhibit a very similar rectangular shape with a coercivity of about 40 mT. The shape of both magneto-optical loops taken at the absorption edges of Co and Ni, reflecting a layer-specific response, closely agrees with that of the loop taken in the visible range, which reflects the collective response of the multilayer system. From this result we can conclude that the entire layer stack undergoes a magnetization reversal as a single magnetic unit. All ferromagnetic layers in the stack are strongly coupled to each other and the coupling across the Si interlayer is of ferromagnetic nature. This ferromagnetic coupling can be a consequence of either intrinsic interlayer exchange coupling, pinholes or other imperfections in this very thin interlayer, which permit a direct ferromagnetic exchange interaction between the magnetic layers. It remains to be seen whether the coercive field is determined by the magnetic properties of the constituent layers or whether it is directly related to the ferromagnetic interlayer coupling.

The center graph in Fig. 4 displays the data taken from a region of the sample where top and bottom magnetic layers are separated by a Si spacer of 2.5 nm. Two distinct steps and a third small step at ±50 mT can be identified in the point symmetric hysteresis loop taken in the visible range. This already points toward a more complex switching behavior, which may be related to a rather individual behavior of the ferromagnetic layers and therefore a weakly coupled state in the multilayer. In the element-selective magneto-optical loops both steps around ±75 mT agree very well with the coercivity of the loops taken at the Ni edge. The second switching event around ±50 mT and the third step around ±15 mT, coincide with steps of the magneto-optical loop taken at the Co edge. This analysis reveals that the Ni film in the Ni/Fe bilayer is magnetically harder and switches at higher magnetic fields. Whether this is an intrinsic property

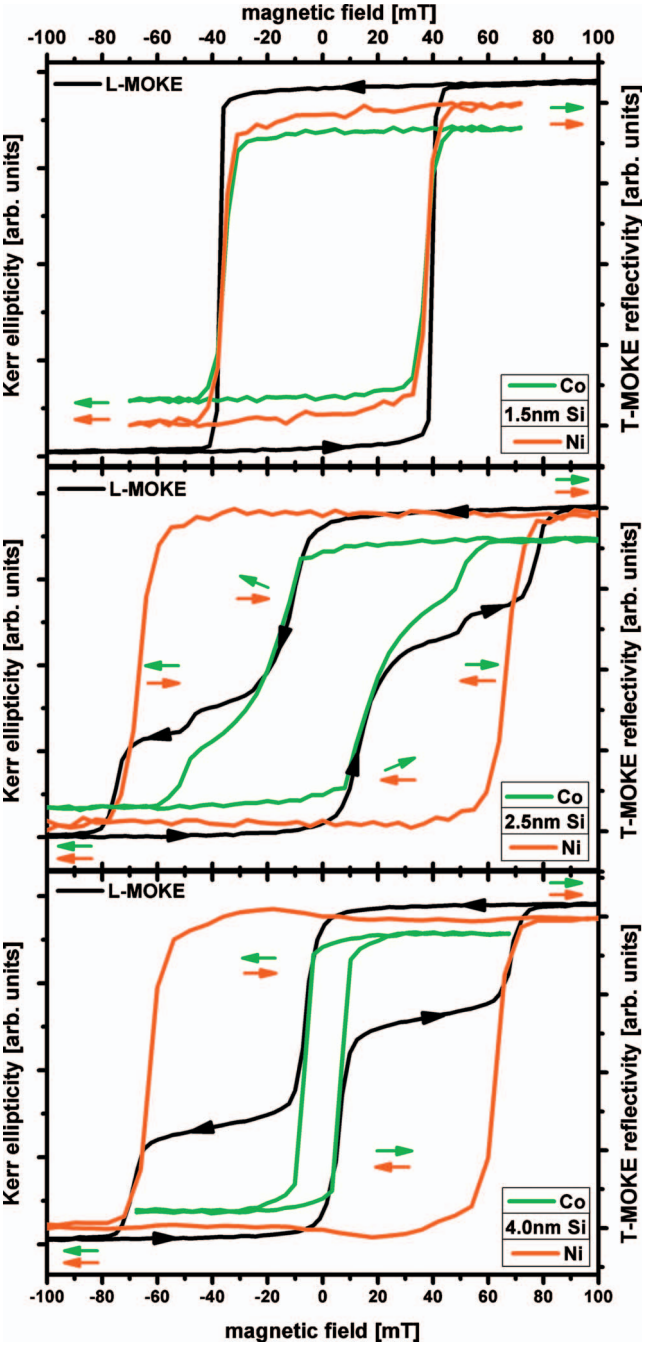

FIG. 4. (Color) Magneto-optical loops of the multilayer wedge system taken at a Si spacer thickness of 1.5 nm (top), 2.5 nm (middle), and 4 nm (bottom).

of the Ni film at that particular thickness, or whether the coercivity is caused by the ferromagnetic coupling to the adjacent Fe layer cannot be distinguished at this point. In any case, it is interesting to note that the larger coercivity of the Ni/Fe bottom layer is not dominating the magnetic response of the sample with strong ferromagnetic interlayer coupling but rather moderately increases the coercivity to a value in between $H_C^{\mathrm{Co}} \approx 15$ mT and $H_C^{\mathrm{Ni/Fe}} \approx 75$ mT.

The bottom graph in Fig. 4 shows loops taken at a region where top and bottom ferromagnetic layers are separated by a Si spacer of 4 nm. Here, the conventional MOKE loop

reveals only two pronounced steps, one of which can be clearly associated with the rectangular magneto-optical loop taken at the Ni absorption edge having a coercivity of $H_C^{\mathrm{Ni/Fe}} \approx 70$ mT. The second step at ± 10 mT in the L-MOKE loop can be clearly related to the switching of the Co layer. This is the typical magnetization loop of a pseudospin-valve system with a negligible magnetic coupling between the hard (Ni/Fe) and soft (Co) magnetic layers.

Summarizing the findings and arguments given above, we can clearly map out the switching behavior of this multilayer system and explore it in detail. For a thin Si spacer, the layer stack is strongly ferromagnetically coupled throughout. The system behaves as one layer, having a coercivity that lies in between the coercivities of the individual decoupled layers, H_C^{Co} and $H_C^{\mathrm{Ni/Fe}}$. The region of the layer stack with a thick Si interlayer is magnetically decoupled allowing for an independent switching of the top and bottom layers. For an intermediate spacer thickness, the top Co layer switches first but it is still weakly coupled to the bottom Ni layer, which governs the switching behavior because of a much higher volume magnetization. This also explains a higher coercivity and a gradual rather than abrupt switching of the Co layer as compared to the decoupled case. Moreover, the system is probably not homogeneous with respect to the coupling strength. This is suggested by the small additional steps in the Co-related loops, which can be found around ± 50 mT. These may be related to areas with an increased ferromagnetic coupling (for example, due to pinholes), which switch at higher magnetic field values.

C. Magneto-optical crosstalk and interferences

It is important to note that layer-selective magneto-optical loops, which can be directly compared with their corresponding classical Kerr effect counterparts, as shown in Fig. 4, can usually be obtained only for a specific set of angles and photon energies. In order to elaborate on this finding, a set of hysteresis loops taken at a fixed angle of 45°, in a photon energy range of 57–68 eV and at a Si spacer thickness of 4 nm is shown in Fig. 5.

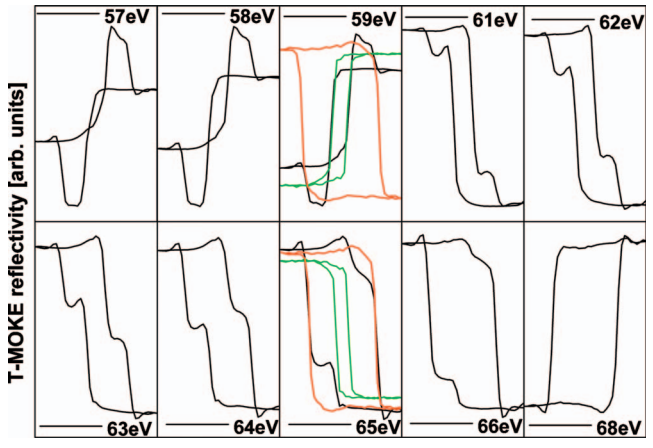

FIG. 5. (Color) Magneto-optical loops taken at an angle of 45°, a Si spacer thickness of 4 nm, and in a energy range of 57–68 eV.

By scanning the photon energy across the Co and Ni absorption edges, the shape of the recorded magneto-optical loops changes significantly. It is striking that all loops are considered to be a linear combination of the pristine loops associated with the individual switching of the Co and Ni layers. Even at local extrema of the magnetic asymmetry, namely, at 59, 61, and 66 eV—compare Fig. 3, supposedly layer-selective magneto-optical loops leave doubt about a decoupled state of the sample.

But this behavior can be understood by first taking into account the switching of the 2 nm thin Fe layer at the very bottom of the multilayer and by second considering the strength and character of the magnetic dichroism at the *M* absorption edges. The Fe and Ni layer, having direct contact to each other, are strongly coupled and switch simultaneously. That is why recording a magneto-optical loop at the Fe and Ni edge would yield the same shape. Due to the energetic proximity of the *M* absorption edges of Fe (54 eV), Co (60 eV), and Ni (67 eV) and the width of the 3*d* bands, the electrons are excited into for magnetic contrast generation, the magneto-optical response of a single element is spread over several electron volt,[14] thereby reaching into the response of a neighboring element. Besides this crosstalk, interferences play a role in the magneto-optical response of the multilayer. As has been outlined above, changing the thickness of the nonmagnetic interlayer can influence the magneto-optical response of individual layers as well as the multilayer as a whole, resulting in an energetic shift of the magnetodichroic signal. As a consequence, the overall magneto-optical response of the Co layer is influenced by the response of the Fe and Ni layer and vice versa resulting in an energy-dependent superposition of the measured magneto-optical loops. Figure 5 and basic calculations reveal, for photon energies below 60 eV, that the measured magneto-optical loops can be reproduced by the weighted *difference* of two rectangular loops associated with the switching of the Fe and Co layers—compare layer-selective loops extracted from Fig. 4 and inserted into Fig. 5 at 59 eV. Whereas for photon energies above 60 eV, the measured magneto-optical loops can be reproduced by the weighted *sum* of two rectangular loops associated with the switching of the Ni and Co layers—compare layer-selective loops extracted from Fig. 4 and inserted into Fig. 5 at 65 eV. Only by recording a loop at the far end of the photon spectrum at 68 eV, it is possible to obtain a pristine magneto-optical loop proofing that the multilayer is magnetizationally decoupled. The weight and relative sign of the magneto-optical loop superposition depends on the magneto-optical constants which can be calculated for each individual layer as well as the entire multilayer system on the basis of the magneto-optical formalism outlined above.[25] And that is also how layer selectivity can be gained at arbitrary sets of angles and energies. Nevertheless, we have demonstrated in the example above that it is preferable to choose the angle of incidence such that the magneto-optical response of individual layers is clearly separated.

VII. SUMMARY AND CONCLUSION

We have measured resonantly enhanced reflection spectra of a polycrystalline Co/Si/Ni/Fe multilayer wedge system in

a T-MOKE geometry across the *M* absorptions edges of Co and Ni. We explored the character of the magnetic dichroism in the XUV and its potential for layer-selective investigations. To this end we studied the magneto-optical response as well as the switching behavior of the Co (5 nm) and Ni/Fe (8 nm, 2 nm) layers as a function of the interlayer coupling by varying the angle of incidence, the photon energy, and the Si spacer thickness.

We showed that the magnetic contrast at the *M* absorption edges of Co and Ni (59.5 eV and 66.5 eV) can be as large as 80% and 25%, respectively, near the Brewster angle in a comfortable 90° reflection geometry. By means of magneto-optical calculations, we were able to show that the shift of local magnetic contrast maxima is related to interference effects in the multilayer system. By recording hysteresis loops for various incidence angles and photon energies, it was possible to characterize the role played by magneto-optical interferences and crosstalk with regard to a layer-selective response of the multilayer stack. This consequently enabled us to understand the switching behavior of individually selected layers as a function of the ferromagnetic interlayer coupling, whose strength decreases with increasing spacer thickness.

Our work lays the basis for element- and layer-selective magnetic investigations in this increasingly interesting spectral range. Especially so, as recently developed table-top soft x-ray sources manage to produce ultrafast and coherent XUV pulses up to photon energies of 100 eV with moderate effort, thus opening the door for element-selective investigations of magnetic properties in heterogeneous systems on the femtosecond and nanometer scale in a laboratory environment.

ACKNOWLEDGMENTS

We would like to thank Bernd Küpper, Jürgen Lauer, Heinz Pfeiffer, Norbert Schnitzler, and Reinert Schreiber for their relentless technical support, without which this work would not have been possible. We also are grateful to the BESSY staff for their assistance in running the beamline 24/7. This work was financially supported by the BMBF (Project No. 05KS7UK1).

[1] B. Hillebrands, *Spin Dynamics in Confined Magnetic Structures* (Springer, Berlin, 2004), Vols. 1–3.
[2] I. Žutić, J. Fabian, and S. Das Sarma, Rev. Mod. Phys. **76**, 323 (2004).
[3] J. Stöhr and H. C. Siegmann, *Magnetism: From Fundamentals to Nanoscale Dynamics* (Springer, Berlin, 2006).
[4] A. Zvezdin and V. Kotov, *Modern Magnetooptics and Magnetooptical Materials* (Institute of Physics, Bristol, 1997).
[5] C. Kao, J. B. Hastings, E. D. Johnson, D. P. Siddons, G. C. Smith, and G. A. Prinz, Phys. Rev. Lett. **65**, 373 (1990).
[6] H.-C. Mertins, D. Abramsohn, A. Gaupp, F. Schäfers, W. Gudat, O. Zaharko, H. Grimmer, and P. M. Oppeneer, Phys. Rev. B **66**, 184404 (2002).
[7] F. Nolting *et al.*, Nature (London) **405**, 767 (2000).
[8] C. Gutt *et al.*, Phys. Rev. B **79**, 212406 (2009).
[9] C. Stamm *et al.*, Nature Mater. **6**, 740 (2007).
[10] F. U. Hillebrecht, T. Kinoshita, D. Spanke, J. Dresselhaus, C. Roth, H. B. Rose, and E. Kisker, Phys. Rev. Lett. **75**, 2224 (1995).
[11] M. Pretorius *et al.*, Phys. Rev. B **55**, 14133 (1997).
[12] M. Sacchi, G. Panaccione, J. Vogel, A. Mirone, and G. van der Laan, Phys. Rev. B **58**, 3750 (1998).
[13] M. Hecker, P. Oppeneer, S. Valencia, H.-C. Mertins, and C. Schneider, J. Electron Spectrosc. Relat. Phenom. **144-147**, 881 (2005).
[14] S. Valencia, A. Gaupp, W. Gudat, H.-C. Mertins, P. M. Oppeneer, D. Abramsohn, and C. M. Schneider, New J. Phys. **8**, 254 (2006).
[15] H. C. Kapteyn, M. M. Murnane, and I. P. Christov, Phys. Today **58**(3), 39 (2005).
[16] X. Zhou, R. Lock, N. Wagner, W. Li, H. C. Kapteyn, and M. M. Murnane, Phys. Rev. Lett. **102**, 073902 (2009).
[17] T. Popmintchev, M. Chen, A. Bahabad, M. Gerrity, P. Sidorenko, O. Cohen, I. P. Christov, M. M. Murnane, and H. C. Kapteyn, Proc. Natl. Acad. Sci. U.S.A. **106**, 10516 (2009).
[18] C. La-O-Vorakiat *et al.*, Phys. Rev. Lett. **103**, 257402 (2009).
[19] R. L. Sandberg, D. A. Raymondson, C. La-O-Vorakiat, A. Paul, K. S. Raines, J. Miao, M. M. Murnane, H. C. Kapteyn, and W. F. Schlotter, Opt. Lett. **34**, 1618 (2009).
[20] K. Starke, F. Heigl, A. Vollmer, M. Weiss, G. Reichardt, and G. Kaindl, Phys. Rev. Lett. **86**, 3415 (2001).
[21] J. E. Prieto, F. Heigl, O. Krupin, G. Kaindl, and K. Starke, Phys. Rev. B **68**, 134453 (2003).
[22] H.-C. Mertins, F. Schäfers, X. Le Cann, A. Gaupp, and W. Gudat, Phys. Rev. B **61**, R874 (2000).
[23] S. Valencia, A. Kleibert, A. Gaupp, J. Rusz, D. Legut, J. Bansmann, W. Gudat, and P. M. Oppeneer, Phys. Rev. Lett. **104**, 187401 (2010).
[24] B. Henke, E. Gullikson, and J. Davis, At. Data Nucl. Data Tables **54**, 181 (1993), released by CXRO (http://henke.lbl.gov/optical_constants/)
[25] S. Valencia, A. Gaupp, W. Gudat, L. Abad, L. Balcells, and B. Martinez, J. Appl. Phys. **104**, 023903 (2008).
[26] R. R. Gareev, D. E. Bürgler, M. Buchmeier, D. Olligs, R. Schreiber, and P. Grünberg, Phys. Rev. Lett. **87**, 157202 (2001).
[27] D. E. Bürgler, C. M. Schmidt, J. A. Wolf, T. M. Schaub, and H. J. Güntherodt, Surf. Sci. **366**, 295 (1996).
[28] M. Buchmeier, R. Schreiber, D. E. Bürgler, and C. M. Schneider, Phys. Rev. B **79**, 064402 (2009).
[29] R. Adam, P. Grychtol, S. Cramm, S. Valencia, and C. M. Schneider (unpublished).
[30] J. P. Hannon, G. T. Trammell, M. Blume, and D. Gibbs, Phys. Rev. Lett. **61**, 1245 (1988).
[31] H. Ebert, L. Baumgarten, C. M. Schneider, and J. Kirschner, Phys. Rev. B **44**, 4406 (1991).
[32] F. Meier and B. Zakharchenya, *Optical Orientation*, Modern Problems in Condensed Matter Sciences Vol. 8 (North-Holland, Amsterdam, 1984).
[33] P. Oppeneer, *Handbook of Magnetic Materials* (Elsevier, Amsterdam, 2001), Vol. 13.
[34] O. Zaharko, P. M. Oppeneer, H. Grimmer, M. Horisberger, H.-C. Mertins, D. Abramsohn, F. Schäfers, A. Bill, and H.-B. Braun, Phys. Rev. B **66**, 134406 (2002).